Sonographic findings of immunoglobulin G4-related sclerosing sialadenitis

Satomi Omotehara[1), 2)], Mutsumi Nishida[1), 2)], Megumi Satoh[2), 3)], Mamiko Inoue[1), 2)], Yusuke Kudoh[1), 2)], Tatsunori Horie[2), 3)], Akihiro Homma[4)], Yuji Nakamaru[4)], Kanako C Hatanaka[5)], Chikara Shimizu[1)]

1. Division of Laboratory and Transfusion Medicine, Hokkaido University Hospital.
2. Diagnostic Center for Sonography, Hokkaido University Hospital.
3. Department of Radiological Technology, Hokkaido University Hospital.
4. Department of Otolaryngology, Hokkaido University Hospital.
5. Department of Surgical Pathology, Hokkaido University Hospital.

Corresponding author: Satomi Omotehara
Address: Division of Laboratory and Transfusion Medicine, Hokkaido University Hospital. N14 W5, Kita-ku, Sapporo 060-8648, Japan
TEL: +81-(0)-11-716-1161
FAX: +81-(0)-11-706-7614
E-mail: s-omote@med.hokudai.ac.jp

Abstract

Purpose

We evaluated the sonographic findings of immunoglobulin G4-related sclerosing sialadenitis (IgG4-SS).

Methods

Nineteen patients with IgG4-SS and 12 healthy volunteers (controls) were enrolled. The following sonographic features were evaluated: 1) enlargement of the submandibular gland by measurement of the longitudinal diameter and thickness; 2) the contour texture of the submandibular gland (smooth or rough); 3) the internal echo texture, categorized into three sonographic patterns (homogeneous, multiple hypoechoic nodule, and diffuse hypoechoic); and 4) quantitative color Doppler signaling.

Results

The longitudinal diameter and the thickness (mean ± SD) of the submandibular gland were significantly greater in patients than in controls ($p=0.005$ and $p<0.001$, respectively). Contour roughness was seen in 62.9% and 8.3% of patients and controls ($p<0.001$), respectively. Homogeneous echo textures alone were seen in controls, whereas multiple hypoechoic nodule patterns were seen in 60% of patients, and diffuse hypoechoic patterns were seen in 40%. Color Doppler signaling (mean ± SD) was significantly higher in patients as compared with controls ($p<0.001$).

Conclusion

Patients could be distinguished from healthy volunteers using four distinctive sonographic findings, suggesting that ultrasonography would be a useful diagnostic tool for IgG4-SS.

Key words: ultrasonography, immunoglobulin G4-related sclerosing sialadenitis, submandibular gland, diagnosis, Doppler signaling

Introduction

Immunoglobulin (Ig) G4-related sclerosing disease is a systemic disease that is characterized by elevated serum IgG4 levels, IgG4-positive plasma cells, and lymphocyte infiltration of various organs [1, 2]. In 2004, Yamamoto et al. confirmed the infiltration of IgG4-positive cells in Mikulicz's disease [3]. In addition, Kitagawa et al. reported that Küttner tumor was an IgG4-related disease [4]. Although Mikulicz's disease and Küttner tumor were formerly thought of as different diseases, serological and histopathological similarities between them have been reported [5]. Both diseases have common clinical features including elevated serum IgG4 levels and histopathologic infiltration of IgG4-positive plasma cells. At present, these diseases are regarded as IgG4-related lesions of the salivary gland [6-9].

There have been some reports of the sonographic features of Mikulicz's disease and Küttner tumors [10, 11]; however, the sonographic features of IgG4-related sialadenitis (IgG4-SS) are not well established. In addition, IgG4-related disease is often difficult to distinguish from malignant tumors of the submandibular gland. Therefore, we evaluated the sonographic features of IgG4-SS.

Material and Methods

Subjects

Between December 2007 and October 2013, 35 glands in 19 patients (11 men, mean age 63 ± 10 years) underwent an ultrasonography examination (US). The diagnosis of IgG4-SS was made when elevated serum IgG4 levels (>135 mg/dL) and diffuse or localized swelling of the submandibular gland were detected, and when marked lymphocyte and plasmacyte infiltration and fibrosis, and infiltration of IgG4-positive plasma cells were seen in histopathologic examination [12]. All of patients were examined by US before administration of prednisolone. In addition, 24 glands in 12 healthy volunteers (controls) including nine men with a mean age of 57 ± 7 years were assessed by US. We analyzed levels of serum immunoglobulin G and immunoglobulin G4 in all study cases.

Procedures

US was performed using a Toshiba Aplio^{TM} XG (with PLT-1204BT and PLT-805AT; Toshiba Medical Systems Corp., Tochigi, Japan), a Logiq 7 (with M12L and 9L; GE Healthcare, Milwaukee, WI, USA) and a Logiq E9 (ML6-15 and 9L; GE Healthcare). We used one of these units with a Toshiba Aplio^{TM} XG for scanning healthy volunteers.

The following features were evaluated: 1) the size of the submandibular gland by measurement of the longitudinal diameter (mm) and thickness (mm); 2) the contour texture of the submandibular gland (smooth or rough); 3) the internal echo texture, categorized into three sonographic patterns including homogeneous, multiple hypoechoic nodule, and diffuse hypoechoic (Fig. 1); and 4) quantitative color Doppler signaling.

We defined the criteria for the three internal echo textures patterns as follows. The homogeneous pattern had no definite hypoechoic area. The multiple hypoechoic nodule pattern showed apparent hypoechoic lesions, regardless of nodule size. If the majority of the gland showed a hypoechoic

pattern, it was classified as the diffuse hypoechoic pattern. If a gland showed both multiple hypoechoic nodule and the diffuse pattern, the dominant pattern was selected. We used a DICOM viewer to analyze the contour and the internal echo texture.

The contour texture and the internal echo textures were reviewed retrospectively in a blinded manner by two sonographers with 5 and 25 years of experience of evaluating superficial organs. In cases of disagreement, the texture pattern was decided by consensus between the sonographers.

The quantitative assessment of color Doppler signaling was undertaken in 40 glands using the Toshiba Aplio^{TM} XG connected to an 8-MHz linear transducer. The pulse repetition frequency was fixed to avoid parameter differences. The color Doppler gain was maximized until disappearance of noise. Color Doppler images were converted into black and white using Adobe Photoshop 5.0J (Adobe Systems Inc, CA, USA), and the ratio of color Doppler signaling to the parenchyma was calculated (mean ± SD, ratios were expressed as percentages).

Statistical analyses

Statistical analyses were performed using the Mann-Whitney U test to compare lesion sizes and color Doppler ratios, and the Chi-square test was used to compare internal echo texture patterns between patients and controls. All statistical analyses were performed using IBM SPSS software version 20.0. A p-value of <0.05 was considered to be statistically significant.

Results

Clinical and US features of the study participants are shown in Table 1. Among patients with IgG4-SS, the serum IgG4 level exceeded the measurement limit (1500 mg/dL) in one patient. Therefore, data from that patient were excluded when determining the mean IgG4 levels. The longitudinal diameter and thickness of the submandibular gland were significantly greater in patients with IgG4-SS than in controls ($p=0.005$ and $p<0.001$, respectively). The majority of patients with IgG4-SS had a rough contour texture, whereas the majority of controls had a smooth contour texture ($p<0.001$). Patients with IgG4-SS showed diffuse hypoechoic or multiple hypoechoic nodule internal echo patterns, whereas all controls had a homogeneous pattern. The mean Doppler signaling ratio was significantly higher in patients with IgG4-SS than in controls ($p<0.001$).

Typical ultrasonograms of the submandibular glands in a control subject are shown in Figure 2. The serum IgG and IgG4 levels in this subject were both within the normal range at 1277 mg/dL and 32.1 mg/dL, respectively. Typical ultrasonograms from a patient with IgG4-SS are shown in Figure 3. The serum IgG and IgG4 levels in this patient were elevated at 2326 mg/dL and 534 mg/dL, respectively. In addition, the ratio of color Doppler signaling was significantly increased in both submandibular glands. A pathological specimen was obtained from the patient by excisional biopsy of the left submandibular gland (Figure 3E–H). Pathological analysis revealed marked fibrosis around acinar structures and obliterative phlebitis. Inflammatory lymphocytes and plasma cells were also seen. The ratio of IgG4-positive to IgG-positive cells was 72%. The region of

lymphoplasmacytic infiltration mostly corresponded to the hypoechoic region on the ultrasonogram. Ultrasonograms of a patient with IgG4-SS showing submandibular glands exhibiting the diffuse hypoechoic pattern are shown in Figure 4. The serum IgG and IgG4 levels in the patient were both elevated at 2761 mg/dL and 143 mg/dL, respectively.

Discussion

In this study, both the longitudinal diameter and thickness of the submandibular glands were significantly greater in patients with IgG4-SS than in controls, and the increase in the thickness was especially remarkable. The typical sonographic features of the submandibular glands in patients with IgG4-SS were rough contours, multiple hypoechoic nodule, or a diffuse hypoechoic pattern, and increased color Doppler signaling ratios. These findings are thought to represent the characteristic appearance of IgG4-SS. The histological characteristics of IgG4-SS have been reported as lymphoplasmacytic infiltration and fibrosis around ducts and lobules with preservation of lobular architecture [13-15], which would be consistent with our IgG4-SS findings in the present study. The contour roughness and high-echoic borders of the multiple hypoechoic nodules might reflect marked fibrosis around lobules and ducts, whereas the diffuse hypoechoic pattern would be consistent with lymphoplasmacytic infiltration.

In some of our cases, distinguishing internal echo patterns was difficult, especially between the diffuse hypoechoic and multiple hypoechoic nodule patterns. Disagreements were recorded in the assessments of 9 out of 35 glands, and we needed to reach consensus. For example, in Figure 3B, although we defined the left submandibular gland as having a diffuse hypoechoic pattern, the gland could easily have been categorized as having the multiple hypoechoic nodule pattern. Because the hypoechoic area in the gland would increase according to the degree of lymphoplasmacytic infiltration, eventually an intermediate pattern would likely exist. However, all submandibular glands in controls showed a homogenous internal echo pattern, so it was still possible to distinguish between IgG4-SS and controls by US.

The increased color Doppler signaling ratio detected in patients with IgG4-SS in the present study was thought to correspond with increased blood flow via existing blood vessels, rather than represent any changes caused by tumor angiogenesis, because blood flow was detected along existing blood vessels, none of which were tortuous or had an aberrant structure. However, increased color Doppler ratios could also be indicative of inflammation.

Asai et al. classified IgG4-SS-related sonography findings into two patterns based on the shape, contour texture, and internal echo texture [16]. Glands that had an almost lobular shape and uneven contours represented the hypoechoic pattern and were considered the tumor-forming type, whereas the diffuse focal type had a preserved shape and normal contours with multiple hypoechoic foci. They reported that, according to histopathological analysis of the specimen, the region of fibrosis was the only difference between the two IgG4-SS types. These sonographic features were similar to those uncovered in the present study.

Enlargement of submandibular glands is also seen in sialolithiasis and malignant tumors, which can make the differential diagnosis of IgG4-SS by US problematic. However, sialolithiasis shows stones

with acoustic shadows in the dilated ducts. Malignant lymphomas, especially mucosa-associated lymphoid tissue lymphoma (MALT lymphoma), show hypoechoic areas with rough or dense linear echogenic strands and a lobulated shape with a markedly hypoechoic internal echo texture in the thyroid and salivary glands [17, 18], making them especially difficult to distinguish from IgG4-SS. However, Asai et al. reported that the sonographic findings of MALT lymphoma included a tortoiseshell pattern with an increased hypoechoic internal echo texture compared with IgG4-related disease [19]. Therefore, it is important to bear in mind that, when making a diagnosis of IgG4-SS, a combination of serological testing and biopsy would be needed for a definitive diagnosis.
A limitation of the present study was that we did not examine any patients with MALT lymphoma during the study period and therefore could not compare the sonographic features of IgG4-SS and MALT lymphoma. Another limitation was that we focused on the amount of color Doppler signaling, but a detailed evaluation of the vascular structure might have been more useful for making a differential diagnosis.

Conclusion

The sonographic features evaluated in the present study could differentiate IgG4-SS from healthy submandibular glands. Sonographic submandibular gland features such as enlargement, a rough contour texture, a diffuse hypoechoic or multiple hypoechoic nodule pattern, and increased color Doppler signaling were all useful indicators for a diagnosis of IgG4-SS.

Conflict of interest: Satomi Omotehara, Mutsumi Nishida, Megumi Satoh, Mamiko Inoue, Yusuke Kudoh, Tatsunori Horie, Akihiro Homma, Yuji Nakamaru, Kanako C Hatanaka, and Chikara Shimizu declare that they have no conflict of interest.

Statement of Ethics: All procedures followed were in accordance with the ethical standards of the responsible committee on human experimentation (institutional and national) and with the Helsinki Declaration of 1964 and later versions. Informed consent was obtained from all subjects included in the study.

References

[1] Kamisawa T, Okamoto A. IgG4-related sclerosing disease. World J Gastroenterol. 2008;14:3948–55.
[2] Stone JH, Zen Y, Deshpande V. IgG4-related disease. N Engl J Med. 2012;366:539–51.
[3] Yamamoto M, Ohara M, Suzuki C, et al. Elevated IgG4 concentrations in serum of patients with Mikulicz's disease. Scand J Rheumatol. 2004;33:432–3.
[4] Kitagawa S, Zen Y, Harada K, et al. Abundant IgG4-positive plasma cell infiltration characterizes chronic sclerosing sialadenitis (Küttner's tumor). Am J Surg Pathol. 2005;29:783–91.
[5] Takano K, Yamamoto M, Takahashi H, et al. Clinicopathologic similarities between Mikulicz disease and Küttner tumor. Am J Otolaryngol. 2010;31:429–34.
[6] Himi T, Takano K, Yamamoto M, et al. A novel concept of Mikulicz's disease as IgG4-related disease. Auris Nasus Larynx. 2012;39:9–17.
[7] Yamamoto M, Takahashi H,Ohara M,et al. A new conceptualization for Mikulicz's disease as an IgG4-related plasmacytic disease. Mod Rheumatol. 2006;16:335–40.
[8] Geyer JT, Deshpande V. IgG4-associated sialadenitis. Curr Opin Rheumatol. 2011;23:95–101.
[9] Kamisawa T, Zen Y, Pillai S, et al. IgG4-related disease. Lancet.2015;385:1460–71.
[10] Shimizu M, Moriyama M, Okazaki K, et al. Sonographic diagnosis for Mikulicz disease. Oral Surg Oral Med Pathol Oral Radiol Endod. 2009;108:105–13.
[11] Ahuja AT, Richards PS, Wong KT, et al. Kuttner tumour (chronic sclerosing sialadenitis) of the submandibular gland: sonographic appearances. Ultrasound Med Biol. 2003;29:913–9.[12] Umehara H, Okazaki K, Masaki Y, et al. Comprehensive diagnostic criteria for IgG4-related disease (IgG4-RD), 2011. Mod Rheumatol. 2012;22:21–30.
[13] Takagi Y, Nakamura H, Origuchi T, et al. IgG4-related Mikulicz'z disease: ultrasonography of the salivary and lacrimal glands for monitoring the efficacy of corticosteroid therapy. Clin Exp Rheumatol. 2013;31:773–5.
[14] Ohta N, Kurakami K,Ishida A, et al. Clinical and pathological characteristics of IgG4-related sclerosing sialadenitis. Laryngoscope. 2012;122:572–7.
[15] Laco J, Ryska A, Celakovsky P, et al. Chronic sclerosing sialadenitis as one of the immunoglobulin G4-related diseases: a clinicopathological study of six cases from Central Europe. Histopathology. 2011;58:1157–63.
[16] Asai S, Okami K, Nakamura, et al. Localized or diffuse lesions of the submandibular glands in immunoglobulin g4-related disease in association with differential organ involvement. J Ultrasound Med. 2013;32:731–6.
[17] Orita Y, Sato Y, Kimura N, et al. Characteristic ultrasound features of mucosa-associated lymphoid tissue lymphoma of the salivary and thyroid gland. Acta Otolaryngol. 2014;134: 93–9.
[18] Bahn YE, Lee SK, Kwon SY, et al. Sonographic appearances of mucosa-associated lymphoid tissue lymphoma of the submandibular gland confirmed with sonographically guided core needle biopsy. J Clin Ultrasound. 2011;39:228–32.
[19] Asai S, Okami K, Nakamura N, et al. Sonographic appearance of the submandibular glands in patients with immunoglobulin G4-related disease. J Ultrasound Med. 2012;31:489–93.

Figure legends

Figure 1. Classification of the internal echo texture of the submandibular gland. (A) Homogeneous pattern. (B) Multiple hypoechoic nodule pattern. (C) Diffuse hypoechoic pattern. Yellow arrows indicate the borders of the submandibular gland. Pink arrows indicate multiple hypoechoic nodules.

Figure 2. Ultrasonograms of a normal submandibular gland. The longitudinal diameter and the thickness of the right submandibular gland are 35.4 mm and 15.6 mm, respectively. (A) The contour is smooth and the internal echo texture shows the homogeneous pattern. (B) The ratio of color Doppler signaling is 0.8 %. Yellow arrows indicate the borders of the submandibular gland.

Figure 3. A case of typical IgG4-SS. Both submandibular glands are swollen. The longitudinal diameter and the thickness of the right and left submandibular glands are 33.3 mm and 19.1 mm, and 32.2 mm and 17.3 mm, respectively. The contour texture is rough on both sides. (A) The right submandibular gland shows the multiple hypoechoic nodule pattern. (B) The left submandibular gland shows the diffuse hypoechoic pattern. (C) The color Doppler signaling ratio in the right submandibular gland is 9.7%, whereas that in the left submandibular gland is 8.3% (D). Yellow arrows indicate the borders of the submandibular gland. Histopathological analysis of an excisional biopsy of the left submandibular gland (E–H). (E) Macroscopic hematoxylin-eosin staining. (F, G) Marked fibrosis can be seen around acinar structures and obliterative phlebitis is apparent. (F) The majority of inflammatory cells were lymphocytes or plasma cells (hematoxylin-eosin; F, magnification ×40; G, magnification ×400). (H) Infiltration of IgG4-positive cells is apparent (immunohistochemical staining with an anti-IgG4 antibody, magnification ×400).

Figure 4. Ultrasonograms of submandibular glands showing the diffuse hypoechoic pattern in a patient with IgG4-SS. The longitudinal diameter and the thickness of the right and left submandibular glands are 35.6 mm and 22.1 mm, and 29.8 mm and 20.3 mm, respectively. Both glands show a smooth contour texture. (A) The right submandibular gland. (B) The left submandibular gland. (C, D) Increased color Doppler signaling can be seen in both glands. Yellow arrows indicate the borders of the submandibular gland.

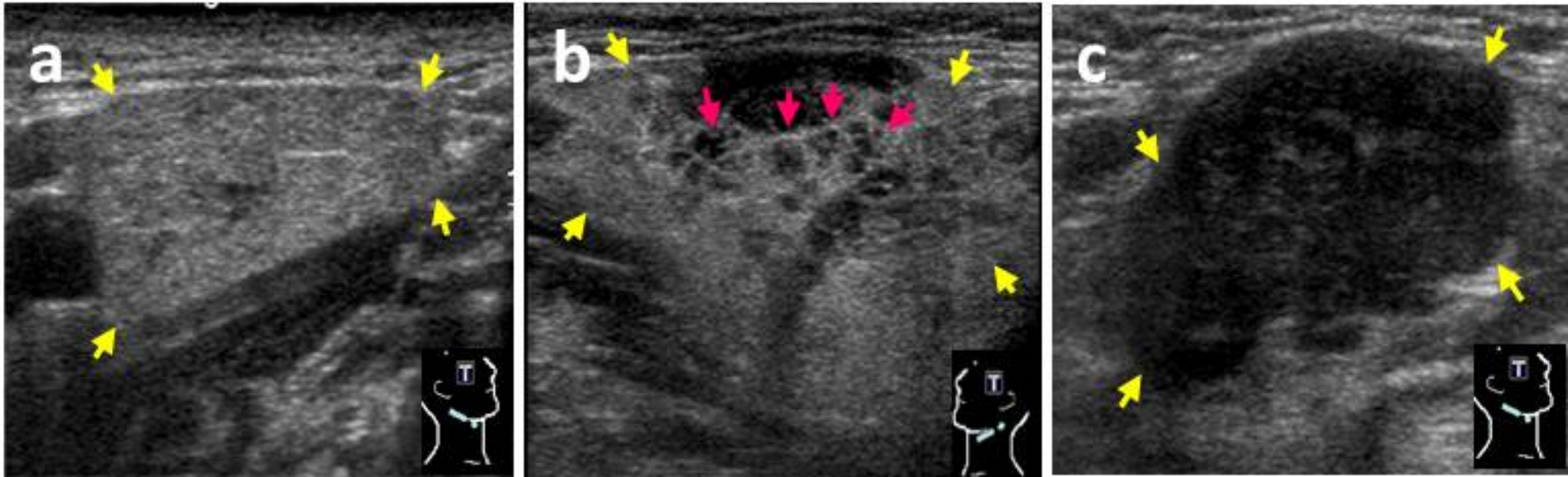
a
b
c

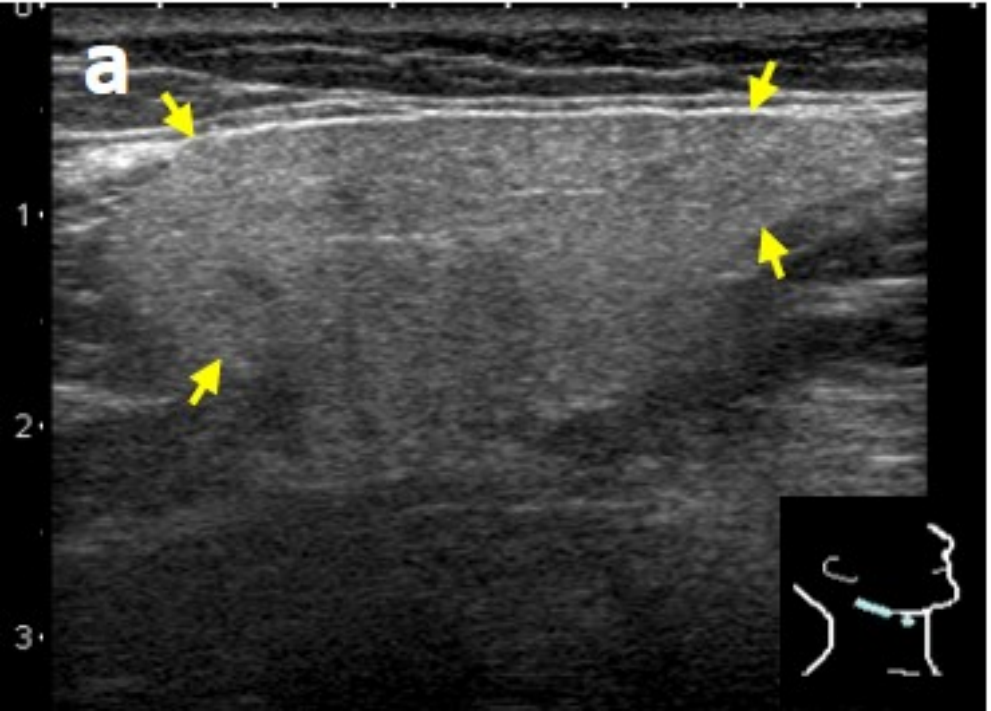
a

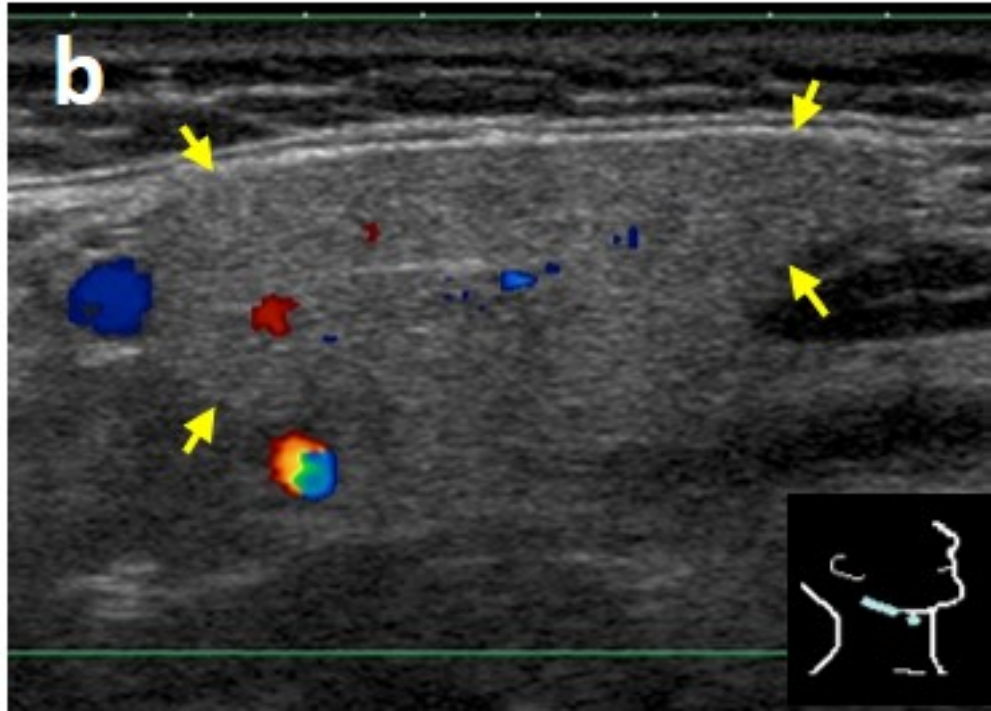
b

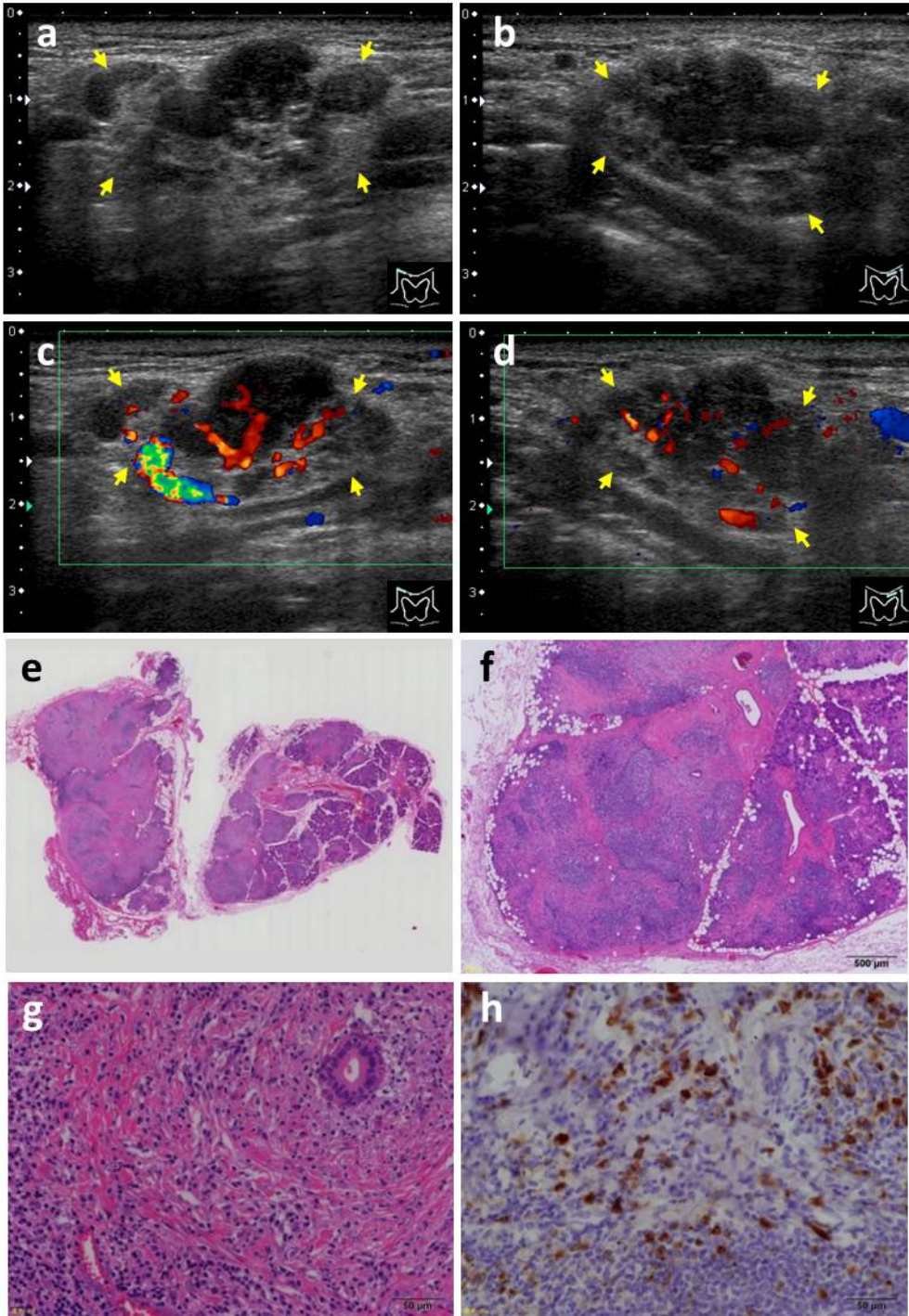
a
b
c
d
e
f
500 µm
g
50 µm
h
50 µm

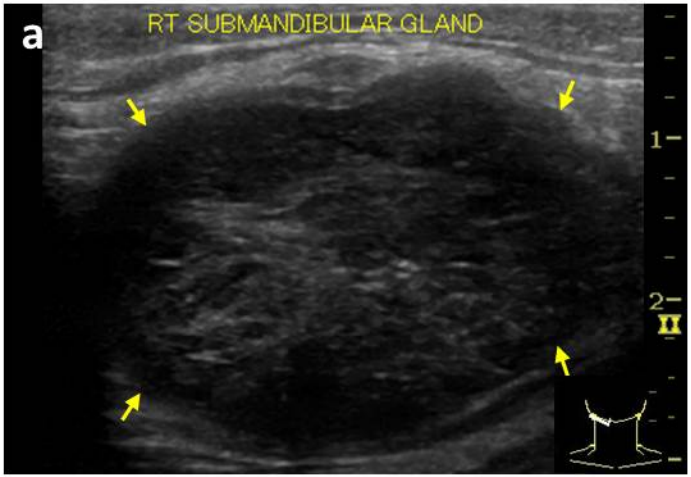
a
RT SUBMANDIBULAR GLAND

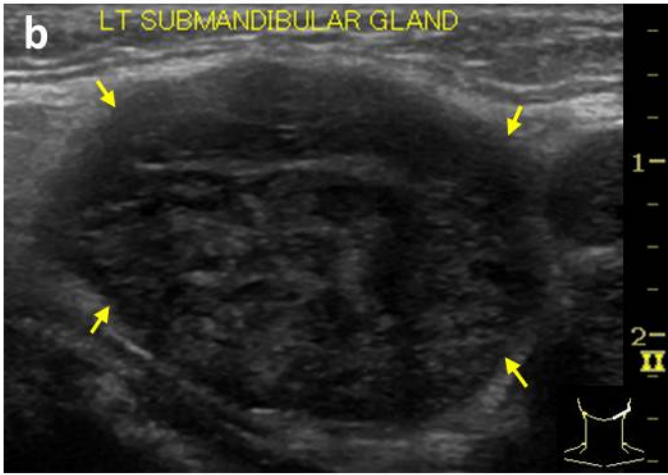
b
LT SUBMANDIBULAR GLAND

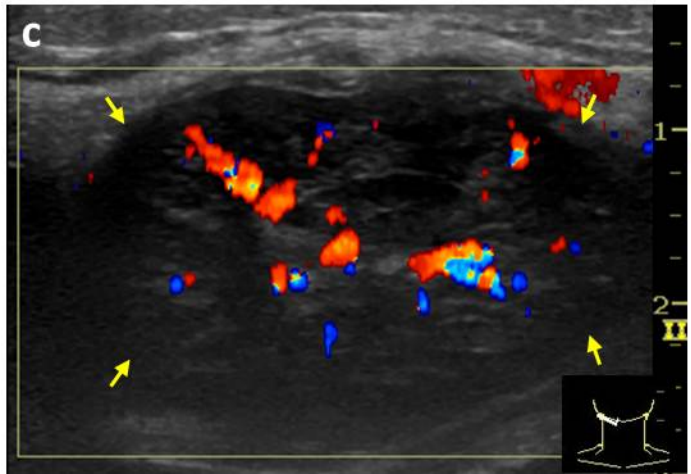
c

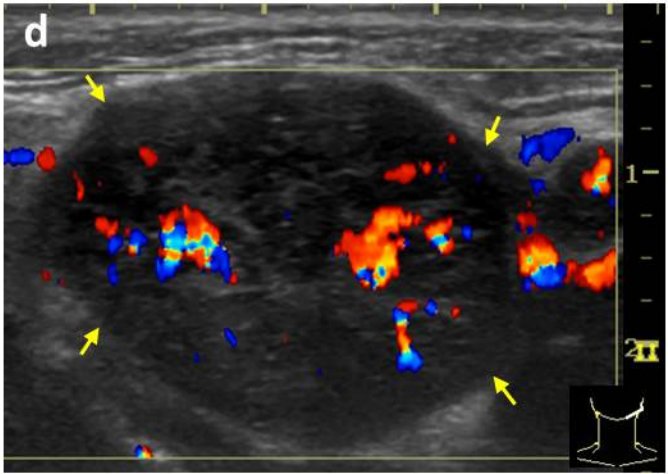
d

Table 1. Clinical and ultrasound feature of the study participants

	IgG4-SS	Healthy Volunteers
n	19	12
Age, years[a]	63±10	57±7
Existence of other organ lesions, n	15	-
Glands, n	35	24
IgG, mg/dL[a]	2478.7±1375.0**	1147.4±271.5
IgG4, mg/dL[a]	743.3±656.4**	61.0±36.6
Longitudinal diameter, mm[a]	37.0±6.2*	32.4±4.0
Thickness, mm[a]	19.3±4.2**	15.1±2.2
Contour, % (n)		
smooth	37.1 (13)	91.7 (22)
rough	62.9 (22)	8.3 (2)
Internal echo texture, % (n)		
homogeneous	0 (0)	100 (24)
multiple hypoechoic nodule	60 (21)	0 (0)
diffuse hypoechoic	40 (14)	0 (0)
Color Doppler signaling ratio, %[a] (n)	9.5±5.3 (16)**	1.6±1.5 (24)

*: $p=0.005$ **: $p<0.001$

[a]Values are mean±SD.